Non-Invasive SAR Using OTA Measurements and Numerical Post Processing

L. Scialacqua[1], S. Anwar[2], F. Mioc[1], A. Lelievre[2], M. Mantash[2], J. Luc[2], N. Gross[3], L.J. Foged[1]

[1] Microwave Vision Italy SRL,Via dei Castelli Romani 59, 00071, Pomezia, Italy, lucia.scialacqua@mvg-world.com

[2] MVG Industries Technopole Best Iroise, Plouzane, France, shoaib.anwar@mvg-world.com

[3] MVG Industries, 13 rue du Zéphyr 91140 Villejust, France, nicolas.gross@mvg-world.com

Abstract— **In the last few years, the use of wireless devices has increased significantly, the evaluation of the Specific Absorption Rate (SAR) is fundamental to comply with human safety regulations. Different methodologies can be used for SAR assessment, crucial parameters are the reduction of testing time and the achievable accuracy. Recently a Non-Invasive SAR evaluation technique based on passive Near-field measurements and numerical assisted post-processing has been studied and validated for a connectorized radiating element [1]. In this paper this technique is applied to an Over The Air (OTA) measurements combined with post processing and numerical simulations of a Golden Wireless Device (GWD). Reference measurements using a standard legacy SAR measurement system have been performed and compared with the proposed technique showing a good agreement. These results validate the approach and confirm the applicability of Non-Invasive SAR as a faster alternative for pre-compliance SAR measurements for modern day communication devices.**

Index Terms— Over The Air, OTA, Specific Absorption Rate, SAR, Golden Wireless Device, LTE, Near-field measurements, Numerical simulations.

I. INTRODUCTION

Non-invasive Fast SAR techniques have been an area of interest since the arrival of 4G in the market [2],[3]. The legacy systems (e.g [4]), with single probe sequentially scanning a liquid inside a phantom to evaluate the maximum E-Field and then the SAR around this hot-spot, take substantial amount of time.

The main idea behind improving the measurement time using fast SAR techniques was to use multiple probes with a wide band liquid phantom and do parallel measurements on a given plane inside the phantom. Combining with smart grid techniques and post-processing, SAR evaluation time was considerably reduced.

The modern-day devices, with the arrival of 5G, Wi-Fi 7, and MiMO technology, and co-existence with legacy technologies, have made the SAR evaluation a very lengthy process. A typical high-end smart phone supports more than 60 frequency bands (2G, 3G, LTE, 5G FR1, 5G FR2, Wi-Fi, Bluetooth, GPS and more recently satellite link frequencies).

For each frequency band and its corresponding modulation, the SAR is evaluated for 1g and 10g tissue volumes, for different use cases and positions (head, trunk) and orientations of the device (left, right, front, back, tilted), and for each corresponding antenna for MiMo case. The latest standard procedures allow for both fast and legacy SAR techniques [5].

In addition to fast SAR techniques, recently a new approach to evaluate SAR has been proposed based on standard near-field measurements of a radiating device (DUT), and equivalent current approach [6]-[10] to evaluate a NF source (in form of Huygens's box) representing the DUT. The SAR is then computed using a full wave simulation by introducing liquid phantoms around the device. For the above described feature the equivalent current approach is particularly efficient when a full wave model of the DUT is not available (this can happen frequently), but the DUT can be measured. The concept is called "Link" approach, which corresponds to the link between measurements and numerical assisted post-processing; it has been validated for a simple dipole as DUT providing close correlation with legacy SAR evaluation approach and full-wave 3D simulations results [1]. The principal advantages of such technique are the following. There is no need to have liquid phantoms. The measurement setup is unique for all frequencies, and this reduces risk of measurement errors. The whole process can be automatized, and risk of mistakes is minimized. The different orientations of phone and phantoms can all be evaluated using full-wave simulations with different separation distances using a parametric approach.

In this paper, the link approach is applied to a MVG's Golden Wireless Device (GWD). The advantage of such a device is that it is representative of a modern smart phone with a known radiating element and repeatable performance. Using over the air (OTA) near-field measurements, the equivalent current source is evaluated for a given frequency and modulation scheme. Using the equivalent current model (Huygens's box) representing the DUT, full-wave 3D simulations are performed with a liquid phantom placed in proximity of the device and the SAR value is obtained. This same DUT is also measured using a legacy SAR measurement system. The results are compared to validate the approach. The link approach assumes that the coupling effects between the DUT and phantom and DUT impedance miss-match are considered with sufficient precision during the full-wave simulations.

The paper is organized as follows. Section II presents the test setup and methodology adopted for this approach and for the legacy SAR system. Results are detailed in Section III. Section IV concludes the study and perspectives are outlined.

II. DESCRIPTION OF THE VALIDATION PROCEDURE

The validation procedure is described in the following paragraphs.

A. The DUT

MVG's Golden Wireless Device (GWD) is the DUT selected for this study as presented in Fig. 1. This device consists of a Wi-Fi modem, and a cellular modem module supporting different communication protocols such as 2G, 3G and LTE. A two-way RF switch controls which modem output to select. The modem outputs are separated into two switched paths, one path has a coaxial connector permitting conducted measurements. The other path is routed to a printed monopole radiating antenna. In addition, a coupler is used with a power detector to measure the power emitted by the modem during the operational period. The device is powered by a Li-ion battery and a microcontroller is used for RF path switching, initializing, and getting information to and from the Modems.

Fig. 1. MVG Golden Wireless Device.

The GWD is conceived for SAR and OTA users who are looking to validate their system. The main advantage of such a device as opposed to a commercially available smart phone, is that there is a full control of modem, radiation pattern, and monitoring the output power. These aspects are critical when calibrating a measurement system and it is not achievable using a commercial smart phone (or golden phone).

The GWD supports various frequency bands (LTE, W-CDMA, GSM, Wi-Fi, etc). For our study two frequencies have been selected with FDD scheme, LTE B3 (UL: 1747.5 MHz, DL: 1842.5 MHz) and LTE B7 (UL: 2535MHz, DL: 2655 MHz).

B. Reference SAR system

MVG's ComoSAR v5 system [4] is selected for the reference measurements with the GWD. The setup is presented in Fig. 2. The system follows the IEC/IEEE 62209-1528 method [5]. The DUT is placed beneath a liquid phantom representing a human trunk. A scalar E-field probe is inserted into the liquid phantom and its position is precisely controlled with a robotic arm. The alignment of the probe and robotic arm is ensured using image processing techniques with the help of a camera.

The phantom liquid represents the electromagnetic characteristics of the human body tissue over the target frequency bands.

The DUT is placed beneath the phantom using a precise positioning system which has negligible impact on the RF performance.

The DUT is controlled using a Radio communication tester (RCT) to setup the maximum power radiation over the target frequency band (in this case LTE B3 and LTE B7 sequentially). A R&S CMW500 RCT is used in this study.

Once the DUT is emitting in the required frequency band with maximum power, the probe scans the phantom and evaluates the E-field over a pre-defined grid. The maximum field point is then identified and SAR for 1g and 10g can be evaluated using the standardized method [5] for the given frequency band, device orientation, use case (or phantom) and separation distance with the phantom.

In this study, three separation distances were considered between the DUT and the phantom. i) 6.2mm, ii) 9.82mm, and iii) 11.2mm. These distances correspond to precision spacers machined to avoid positioning errors.

MVG OpenSAR software is used to get the E-field data and post-processing for SAR evaluation. Fig. 3 presents an example of scan data and SAR value obtained for LTE B3.

The uncertainty budget of the COMOSAR system is reported in TABLE I.

TABLE I. UNCERTAINTY EVALUATION FOR SAR TEST (MEASUREMENT SYSTEM)

	1g $u_i(\pm \%)$	10g $u_i(\pm \%)$
Expanded Uncertainty (95% CONFIDENCE INTERVAL)	19.02	18.41

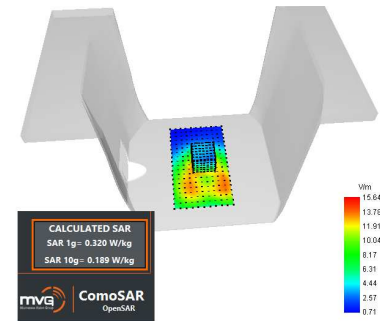Fig. 2. GWD radiating in proximity of a phatom system in the MVG ComoSAR system [4].

Fig. 3. Example of E-field scan and SAR evaluation using MVG OpenSAR software for the MVG Golden Wireless Device (GWD) for LTE B3.

C. Link

The approach of the link consists of the full wave simulation of the device real model (NF source) installed in proximity of the phantom. From the measured radiation pattern of the GWD, NF source or an Huygens's box is evaluated in terms of equivalent currents by the inverse source method [6]-[10] implemented in [11]. The procedure to prepare the NF source is illustrated in Fig. 4 (step 1-3). The behaviour of NF source integrated in the final environment is computed by CST [12] (final step of Fig. 4). Any other commercial full-wave tool could be used for this numerical simulation.
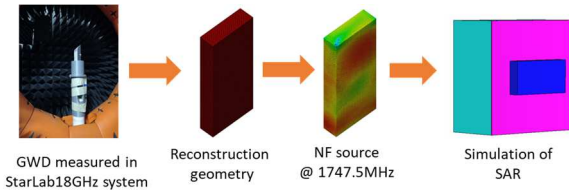

Fig. 4. Working procedure for the link of measurement and simulation.

The first step of the above mentioned procedure is the OTA measurement of the GWD that for this investigation is tested in the StarLab18GHz system [13], shown in Fig. 5. The phase of the measurement is retrieved with a Phase Recovery Unit (PRU). The PRU coupled with the RCT allows to perform OTA measurements and to compute a Near-Field to Far-Field transformations. A scheme of the measurement system working with the PRU for phase recovery is shown in Fig. 6. The RCT and the GWD are the ones used for reference SAR measurements described in the previous section.
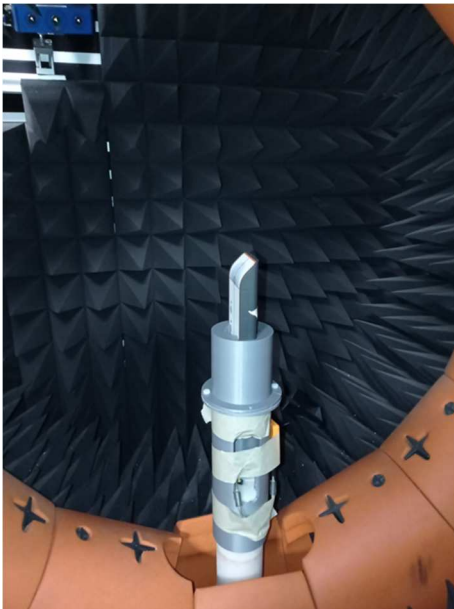

Fig. 5. GWD in the StarLab18GHz – OTA measurement.

Then the second step of the procedure is the preparation of the NF source from the measured Spherical Near Field (SNF).
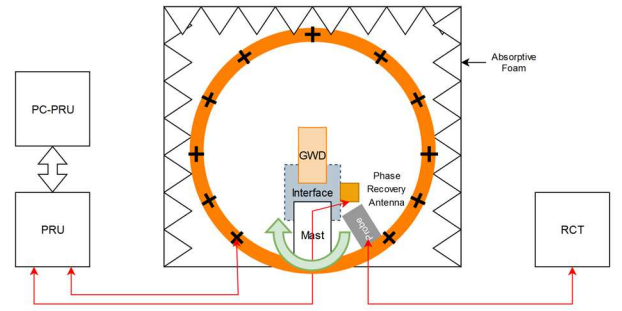

Fig. 6. Scheme of the measuremenst system with a Phase Recovery Unit (PRU) and Radio Communication Tester (RCT).

SNF has been imported and post processed by MVG's Insight tool [11] to generate the NF source model. The geometry is a box and dimensions are 25mm x 79mm x 177mm. The reconstruction geometry and the J electrical current distribution are shown in Fig. 7. The dynamic scale of J-currents is 30 dB, and it can be noted a peak of the currents in correspondence of the location of the main conductors of the antenna. The Signal to Noise Level (SNL) of the reconstructed currents with respect to the measured NF is of the order of -30dB [11].
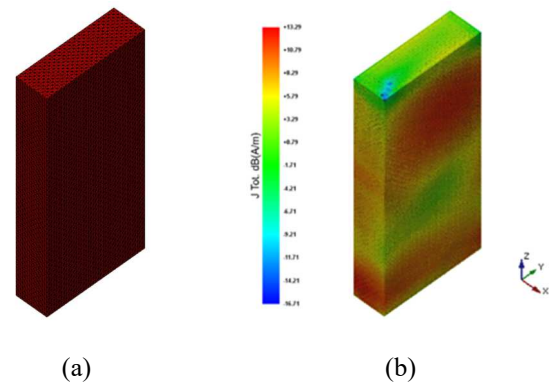

(a)   (b)

Fig. 7. GWD post processed by MVG's Insight tool [11]; (a) reconstruction geometry, (b) J electrical current B3 - 1747.7 GHz.

The final step of the link is the full-wave simulation of the equivalent current source with the phantom, which system characteristics are summarised in TABLE II. They are congruent with the specifications of the phantom model used for of the measurement with MVG ComoSAR V5.

TABLE II. PHANTOM SYSTEM CARACTERISTICS IN THE SIMULATION AT THE TESTED FREQUENCIES

Phantom (X xY x Z)	300 x 300 x 2 mm
Liquid (X xY x Z)	300 x 300 x 150 mm
ε phantom	3.5
ε fluid	40
concductivity fluid	1.4 [S/m]
Density fluid	1000 [kg/m^3]

The separation distances and placement of the current source is the same as for the reference SAR measurements, described in the previous section. The contact position cannot be simulated using the link method due to the minimum distance of a single mesh step ($\lambda/20$) between the real DUT surface and the equivalent current surface.

The setup of the numerical calculation is shown in Fig. 8 for a separation distance of 11.2 mm. The simulated power is set to the value of NF source power. Thus, it is assured that there is no power difference between measurement and simulation.
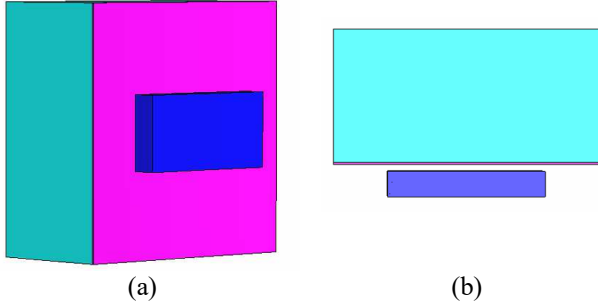

Fig. 8. Simulation of the GWD measured NF model in proximity of the phantom system (phantom in pink and liquid in sky blue); (a) proprestive view (b) lateral view.

For this kind of application, a simplified model of the GWD has been introduced inside the NF source model to include the scattering from the antenna structure. This ensures a better approximation of the real behaviour of the antenna improving the simulation accuracy.

III. VALIDATION RESULTS

The values of the SAR from the reference measurement in the ComoSARv5 system and the approach with the link are reported in TABLE III. and TABLE IV. for 1gr and 10gr, @1747.5MHz and 2535MHz respectively.

TABLE III.   SAR VALUES @1747.5MHz

W/KG (1 GR)				
Distance (d) mm	Reference measurement	Link	Deviation [%]	Deviation [dB]
6.2	0.320	0.286	11%	-0.489
9.82	0.192	0.218	-14%	0.562
11.2	0.171	0.198	-16%	0.637
W/kg (10 gr)				
Distance (d) mm	Reference measurement	Link	Deviation [%]	Deviation [dB]
6.2	0.189	0.188	1%	-0,026
9.82	0.122	0.143	-18%	0.702
11.2	0.109	0.130	-19%	0.766

TABLE IV.   SAR VALUES @2535MHz

W/KG (1 GR)				
Distance (d) mm	Reference measurement	Link	Deviation [%]	Deviation [dB]
6.2	0.158	0.109	31%	-1.607
9.82	0.099	0.081	18%	-0.854
11.2	0.082	0.073	11%	-0.488
W/kg (10 gr)				
Distance (d) mm	Reference measurement	Link	Deviation [%]	Deviation [dB]
6.2	0.080	0.068	14%	-0.678
9.82	0.050	0.051	-3%	0.116
11.2	0.042	0.046	-10%	0.433

The maximum deviation between the reference measurement and the approach of the link is 11% (1gr) / 19% for (10gr) @ 1747.5MHz and it is 31% (1gr) /14% (10gr) @ 2535MHz.

IV. CONCLUSION

In this paper, a continuation of the validation of the Non-Invasive SAR evaluation technique based on passive Near-field measurements and numerical assisted post-processing has been performed using OTA measurements. A MVG's Golden Wireless Device (GWD) has been selected as DUT for the link approach and reference measurements using a standard legacy SAR measurement system (MVG's ComoSAR v5 system).

The agreement between the proposed technique and the measured reference is satisfactory, hence 11% (1gr) / 19% for (10gr) @ 1747.5MHz and it is 31% (1gr) /14% (10gr) @ 2535MHz. These results are coherent / better than the ones published in a similar study recently [14].

This study completes the validation of the proposed approach also for OTA measurement. The accuracy of the technique is then well quantifiable, making this method highly useful to the community for pre-compliance SAR measurements for modern day communication devices.

REFERENCES

[1] L. Scialacqua, S. Anwar, J. F. Mioc, J. Luc, A. Lelievre, M. Mantash, N. Gross, L.J. Foged, "Experimental Validation of Non-Invasive SAR Evaluation from Measurements and Numerically Assisted Post Processing", *2022 Antenna Measurement Techniques Association Symposium (AMTA)*, 2022.

[2] R. Butet *et al*., "Easy to use real time SAR measurements system," *2013 7th European Conference on Antennas and Propagation (EuCAP)*, 2013, pp. 1559-1560.

[3] ART-MAN SAR system from Art-Fi, 2013, https://www.art-fi.eu/art-fi/about-art-fi/about-art-fi2020.

[4] MVG ComoSAR V5 measurement system, https://www.mvg-world.com/fr/produits/sar/sar-systems/comosar-v5.

[5] IEC/IEEE 62209-1528:2020, "Measurement procedure for the assessment of specific absorption rate of human exposure to radio frequency fields from hand-held and body-worn wireless communication devices - Human models, instrumentation and

procedures (Frequency range of 4 MHz to 10 GHz)", published 19th October, 2021.

[6] J. L. Araque Quijano, G. Vecchi, "Improved accuracy source reconstruction on arbitrary 3-D surfaces," Antennas and Wireless Propagation Letters, IEEE, 8:1046–1049, 2009.

[7] J. L. A. Quijano, G. Vecchi, L. Li, M. Sabbadini, L. Scialacqua, B. Bencivenga, F. Mioc, L. J. Foged, "3D spatial filtering applications in spherical near field antenna measurements," AMTA 2010 Symposium, October, Atlanta, Georgia, USA.

[8] L J. Foged, L. Scialacqua, F. Saccardi, F. Mioc, "Measured Antenna Representation of Flush Mounted Antennas for Computational Electromagnetic Solvers," 10th European Conference on Antennas and Propagation, EuCAP, April 2016, Davos, Switzerland

[9] G. L. J. Foged, L. Scialacqua, F. Saccardi, F. Mioc, G. Vecchi. J. L. Araque Quijano, "Antenna Placement based on Accurate Measured Source Representation and Numerical Tools," IEEE Antennas and Propagation Society International Symposium, July 19-24, 2015.

[10] L. J. Foged, L. Scialacqua, F. Saccardi, F. Mioc, D. Tallini, E. Leroux, U. Becker, J. L. Araque Quijano, G. Vecchi, "Bringing Numerical Simulation and Antenna Measurements Together," IEEE Antennas and Propagation Society International Symposium, July 6-11, 2014.

[11] https://www.mvg-world.com, INSIGHT softwave, Microwave Vision Group (MVG).

[12] https://www.3ds.com, CST STUDIO SUITE, Dassault Systems.

[13] https://www.mvg-world.com/en/products/antenna-measurement/multi-probe-systems/starlab, MVG StarLab datasheet.

[14] B. Derat et al., "Base Station Specific Absorption Rate Assessment Based on a Combination of Over- The-Air Measurements and Full-Wave Electromagnetic Simulations," *2021 Antenna Measurement Techniques Association Symposium (AMTA)*, 2021, pp. 1-6, doi: 10.23919/AMTA52830.2021.9620622.